Published in IET Generation, Transmission & Distribution
Received on 7th September 2009
Revised on 26th February 2010
doi: 10.1049/iet-gtd.2009.0505

Special Issue on Wide Area Monitoring, Protection and Control

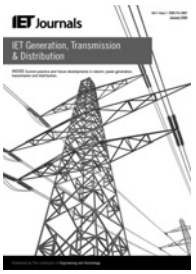

ISSN 1751-8687

Wide area control for improving stability of a power system with plug-in electric vehicles

P. Mitra G.K. Venayagamoorthy

Real-Time Power and Intelligent Systems (RTPIS) Laboratory, Missouri University of Science and Technology, MO 65409, USA
E-mail: gkumar@ieee.org

Abstract: The integration of plug-in electric vehicles (PEVs) to power systems has impacts on the stability characteristics of the integrated systems. Wide area controllers (WACs) are used in power systems to provide auxiliary control signals to the generators or other devices in order to improve the stability of the system. The necessity of WACs becomes more relevant during grid-to-vehicle (G2V) or vehicle-to-grid (V2G) power transactions, that is, charging and discharging cycles of the PEVs respectively. The design of a WAC for providing damping to three generators in a 12-bus power system with PEVs is presented in this study. Each WAC signal is obtained based on the aggregation of modulated local and remote power system stabilisers' signals. The modulation indices associated with those signals are tuned using the particle swarm optimisation technique to provide the maximum damping to the three generators. The 12-bus power system with the PEVs and WAC has been implemented on the real-time digital simulator (RTDS). Typical results have been presented to show the improvement in the stability of the power system when PEVs are integrated using transient simulations and Prony analysis.

1 Introduction

As increasing numbers of plug-in electric vehicles (PEVs) enter the market, the effects of adding large numbers of small power electronic devices to the grid become more and more predominant. Many of these vehicles can also be adopted to participate in vehicle-to-grid (V2G) applications in the proposed smart grid framework which calls for increased amount of bidirectional power flows between vehicles and utility grids [1, 2]. Vehicles providing auxiliary services coordinate their power flows with the utility to change grid conditions in some predetermined way. If vehicle owners try to buy and sell power according to varying prices, there will be large swings in power as groups of vehicles switch the direction of their power flows. Therefore the PEVs are going to have significant impact on the stability of the power grids.

Several measures have been taken in the recent decades to provide better stability and reliability to the stressed systems. Local compensators like power system stabiliser (PSS) are installed to damp out low-frequency oscillations. But, it is observed that the local controllers have good performance when local measurements provide all the information about the dynamics of disturbances. But, if there are adverse interactions between multiple adjacent areas of the power system, or between the grid and the power electronics devices associated with the distributed generations or storage, only a wide-area measurement-based controller can provide better stabilising control [3, 4]. Wide-area controllers (WACs) coordinate the actions of the distributed agents using supervisory control and data acquisition, phasor measurement unit or other sources providing wide-area dynamic information [5, 6]. The WAC receives information/data of different areas in the power system and based on some predefined objective function, sends appropriate control signals to distributed agents for enhancing system's dynamic performance [7].

Several researchers have contributed in the area of wide area monitoring and control. A hierarchical WAC for damping post-disturbance oscillations has been reported in [8]. The other control strategies based on linear matrix inequality [9], gain scheduling and H^{∞}-based control [10, 11] have also been used to provide effective auxiliary

© The Institution of Engineering and Technology 2010

damping control. Wide-area signals-based intelligent control of flexible AC transmission systems devices have been presented in [12, 13]. Most of these studies mentioned so far considered conventional power systems and some of them included renewable sources like wind farms [13]. However, the effects of bidirectional power flows introduced by PEVs on the stability of a power system and the role of WAC in improving the damping of the integrated system are not yet reported.

In this study, the impacts of charging and discharging cycles of the PEVs connected to a 12-bus power system on the stability of the integrated system is presented. An optimal WAC for providing damping signals to the individual generators is designed based on the weighted sum of the local and global stabilising signals using the particle swarm optimisation (PSO) technique. The 12-bus power system, PEVs and the designed WAC are implemented in real time on the real-time digital simulator (RTDS). The design (tuning of the modulation indices) of the WAC is carried out on a digital signal processor (DSP) interfaced with the RTDS. The results with and without the WAC for moderate disturbances like a sudden discharging of the PEVs and also for some extreme situations like a sudden transition from discharging to charging mode or a three-phase fault during a peak charging or discharging cycle are presented in this paper. The real-time simulation results and its Prony analysis show that with the PEVs connected to the power system, the WAC improves the stability of the integrated system significantly.

The primary contributions of this study are:

- Demonstration of a real-time simulation of an integrated power system (fleet of PEVs connected to a power system).
- Illustrating the impacts of PEVs operations and grid faults on the stability of an integrated power system.
- The design and real-time implementation of a WAC for improving the stability of an integrated power system.

2 Power system with PEVs

In order to illustrate the impact of PEVs and the role of WAC in power systems, the 12-bus multi-machine power system [14] is modified as shown in Fig. 1. The 12-bus system has four generators and three interconnected areas. Generator G1 represents the infinite bus. In a typical city, there will be several PEV-distributed parking lots in distances of one to few kilometres. In order to model this,

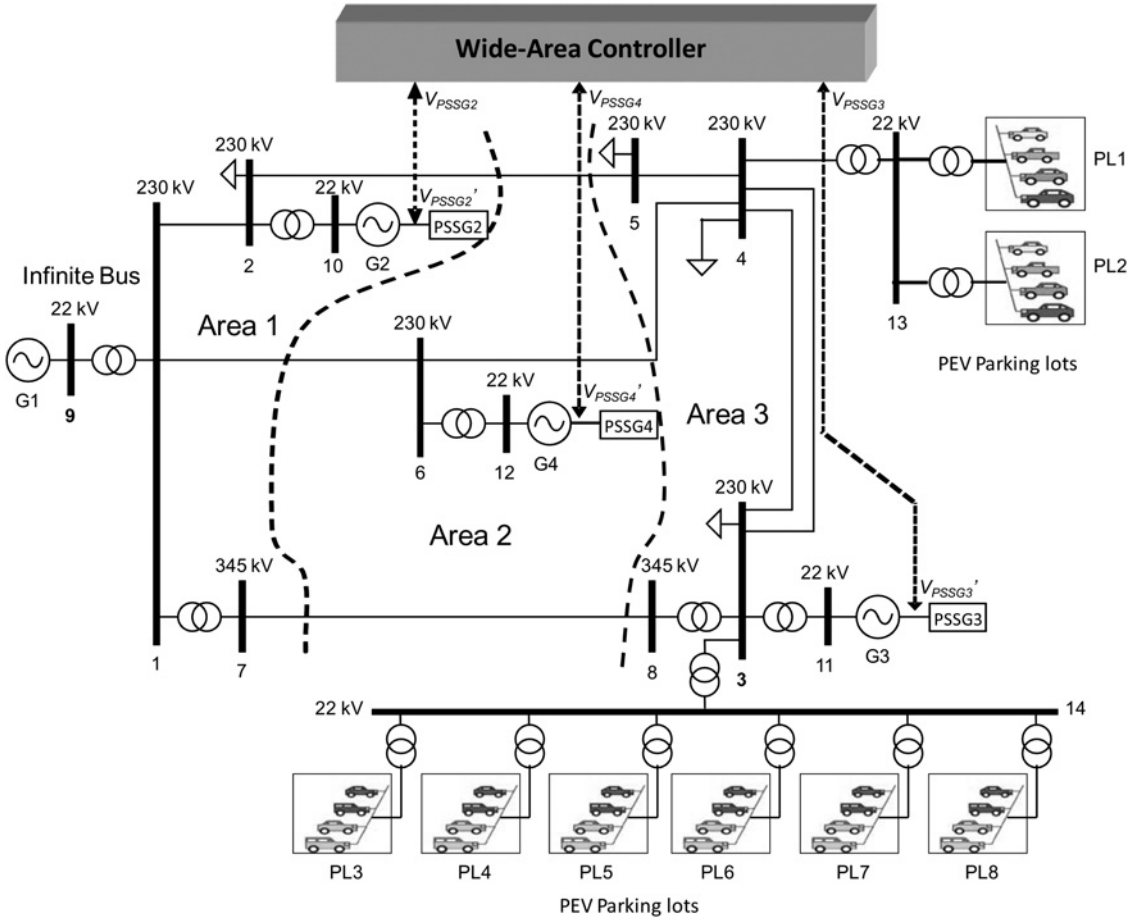

Figure 1 *Twelve-bus test system with PEV parking lots*

© The Institution of Engineering and Technology 2010

doi: 10.1049/iet-gtd.2009.0505

eight three-phase PEV parking lots are added to this system in area 3 (high-load area in 12-bus system). Each parking lot is represented by a DC voltage source followed by a bidirectional three-phase inverter. The inverters are tied to the respective buses through step-up transformers (2.08 kV/22 kV) as shown in Fig. 1. Two of the parking lots, PL1 and PL2, are connected to bus 13 and the remaining six (PL3–PL8) are connected to bus 14. Bus 13 and bus 14 are the two additional buses added to the original 12-bus system in order to connect the PEV parking lots. Buses 13 and 14 are connected to buses 4 and 3, respectively, through 22 kV/230 kV step-up transformers. The control of the inverters is designed in such a way that each parking lot inverter can draw ± 20 MW of active power. Considering each vehicle can draw ± 25 kW, each parking lot in this study represents roughly 800 vehicles aggregated together. Here '+' sign means the vehicles are selling power to the grid, that is, they are in discharging mode and the '−' sign indicates that they are buying power from the grid, that means the vehicles are in charging mode. The entire system is modelled on a RTDS platform [15]. All the parameters of the original 12-bus system are given in [14]. In this study, generators G2–G4 are equipped with PSSs. The PSS parameters are taken from [13] and are listed in Table 1.

The simulation of the inverters on PEVs is carried out using smaller time steps RTDS giga processor (GPC) cards. The GPC is a powerful computational unit which can be used for solving the overall network solution as well as auxiliary components. The GPC contains two IBM PowerPC 750GX RISC processors each operating at 1 GHz. In addition to the network solution and the simulation of standard components at 50 μs time step, the GPC card provides small time step (<2 μs) simulations for voltage source converters. This increase in accuracy allows for better representation of the switching components in a real-time environment. The inverters are designed to operate at 2.08 kV using a three-phase two-level topology and are controlled using a compensation controller [16].

The PEV parking lot configuration presented in the study will become realistic when the vehicle owners will be allowed to participate in the electricity market based on the real-time pricing information. In that case, the vehicle owner can entitle the parking lot owner to use his/her car for buying and/or selling power from/to the grid, respectively, instead of keeping it idle throughout the day in the parking lot. Intelligent methods can be used to find out the near optimal times to buy and sell power from/to the grid to maximise the revenues and minimise emissions for the vehicles participating in V2G operations [17, 18]. Based on that, a pattern will definitely emerge for the charging and discharging operations of the PEV parking lots. There will be times, when most of the vehicles will try to sell power to the grid if the price is high in order to maximise their profit. Similarly, when the price is low, most of the vehicles will try to charge their batteries to its maximum capacity. These are the two extreme cases, when the V2G operation will have the most severe impact on the grid. Also, the V2G parking lots can be used as small power plants and in such cases bulk power transfer in hundreds of megawatts is possible. It is therefore necessary to study the impacts of such bulk transactions on the electricity grid and take necessary measure for improvement of stability.

The design and operation of the WAC block in Fig. 1 is described in Section 4.

Table 1 Local PSS parameters

	PSS at G2	PSS at G4	PSS at G3
K_{STAB}	8	10	12
T_w	10	10	10
T_1	0.2	0.28	0.29
T_2	0.05	0.05	0.06
T_3	0.2	0.28	0.29
T_4	0.05	0.05	0.06

3 Impact of PEVs on the power system stability

In order to study the impact of PEVs on the multi-machine power system described above, two case studies are performed. First, a case where most of the PEVs suddenly switch to the selling (discharging) mode, resulting in a situation where the parking lots connected to buses 13 and 14 inject a total of 30 and 90 MW of active power into the grid, respectively, is simulated. Owing to this sudden flow of 120 MW of active power into the grid, there is a change in the voltage at the point of common coupling of the parking lots. The generator speeds also start oscillating because of this sudden change in the operating points of the various generators in the system. The impact of this sudden discharging of the PEV parking lots can be observed from the speed oscillations of generators G2–G3 as shown in Figs. 2*a*–*c*, respectively. Figs. 2*a*–*c* show comparison of the speed oscillations with and without local PSS connected to the respective generators. It is observed that the PSSs damp out generators' speed oscillations and improve the stability of the integrated system.

In a second case study, an extreme condition is simulated by considering a sudden change of the parking lots' mode of operation from selling to buying. In the previous case, the parking lots were selling a total of 120 MW to the grid. But now they are buying 120 MW from the grid. Owing to the large variations in the operating points of the generators, the speed oscillations with and without PSSs are observed as shown in Figs. 3*a*–*c*. It is observed again that the damping is improved with the local PSS for all the generators G2–G4.

© The Institution of Engineering and Technology 2010

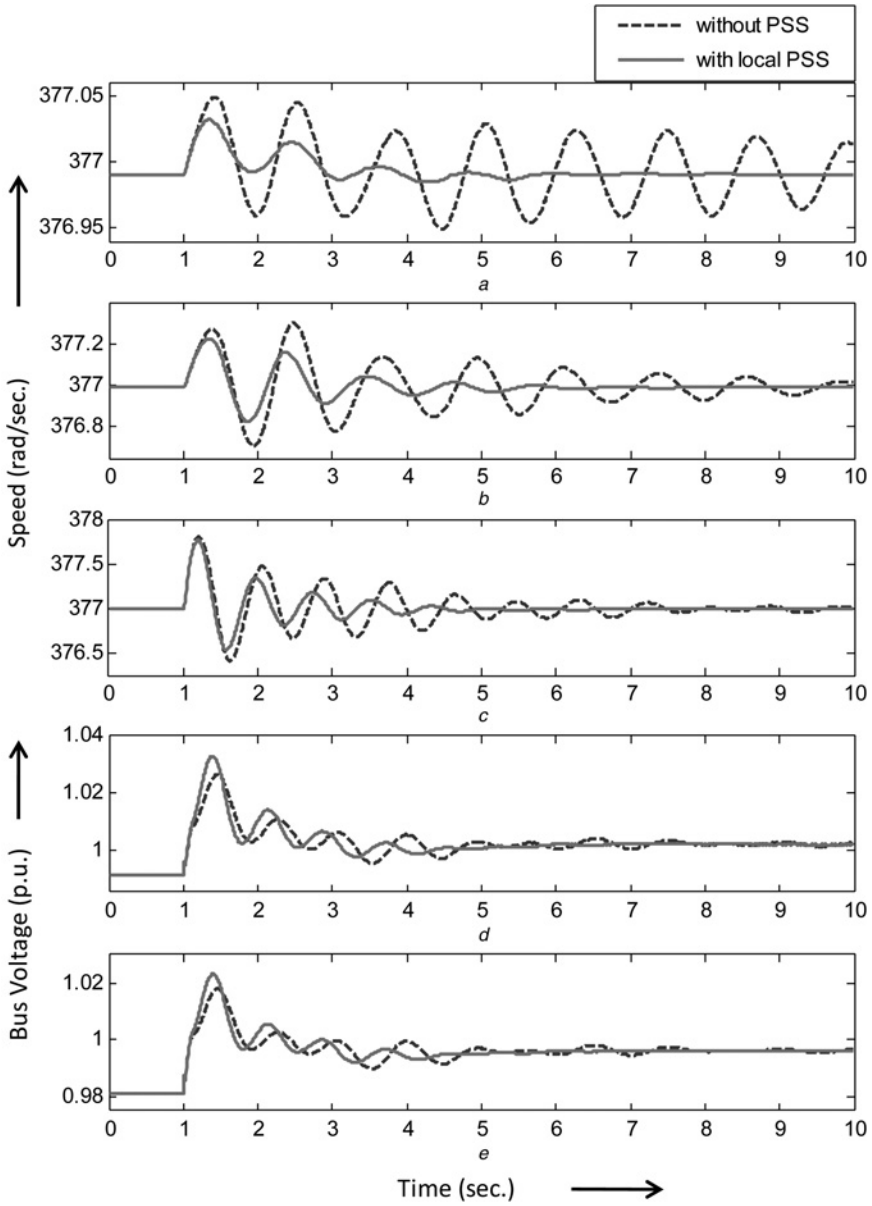

Figure 2 *Impact of sudden discharging of the PEV parking lots with and without PSS*

a Speed oscillation of G2
b Speed oscillation of G4
c Speed oscillation of G3
d Voltage oscillation at bus 14
e Voltage oscillation at bus 13

Figs. 2*d* and *e* show the voltages at the points of common coupling of the PEV parking lots connected to buses 14 and 13, respectively, for the first case of sudden discharging. Similarly, Figs. 3*d* and *e* show the buses 14 and 13 voltages for the second case mentioned above. In Figs. 2*d* and *e*, it is observed that the bus voltage is elevated from 0.98 to 0.995 p.u. at bus 13 and from 0.985 to 1.0 p.u. at bus 14. This is due to the fact that the PEV parking lots injected active power to the buses. Similarly, in Figs. 3*d* and *e*, when the PEVs suddenly switched from discharging to charging mode, the voltage at bus 13 dropped to 0.955 p.u. and voltage at bus 14 dropped to 0.97 p.u. because of the additional 120 MW load at the buses. In Figs. 2*d* and *e*, 3*d* and *e*, it is observed that with PSS on the generators, the voltage oscillation settles down quicker than without PSSs case.

4 Design of WAC

4.1 Structure of WAC

The structure of a standard local PSS is shown in Fig. 4*a*. It has a stabiliser gain, washout filter and two lead-lag compensator blocks. The function of the local PSS is to generate an auxiliary voltage signal V_{PSS} which is to be added to the automatic voltage regulator (AVR) and exciter

© The Institution of Engineering and Technology 2010
IET Gener. Transm. Distrib., 2010, Vol. 4, Iss. 10, pp. 1151–1163
doi: 10.1049/iet-gtd.2009.0505

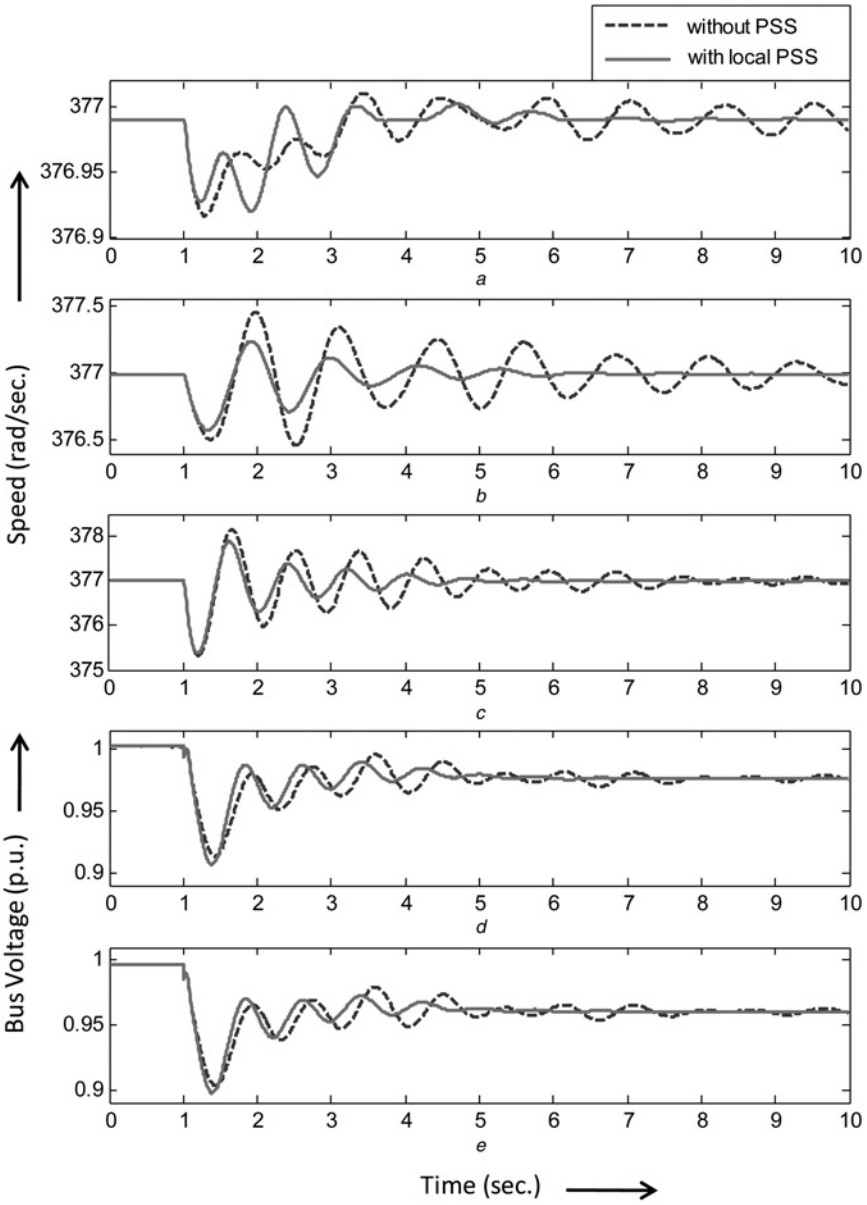

Figure 3 *Impact of sudden transition from discharging to charging of the PEV parking lots with and without PSS*

a Speed oscillation of G2
b Speed oscillation of G4
c Speed oscillation of G3
d Voltage oscillation at bus 14
e Voltage oscillation at bus 13

input based on the speed deviation signal ($\Delta\omega$) of the generator. The PSS parameters can be tuned to damp a specific frequency of oscillation representing some local mode of interest. The problem with these local PSSs is that they have no information about the other areas of the system, the nature of disturbance faced by the other generators and also the control action taken by the remote PSSs. The essence of wide area monitoring and control is to provide local damping controllers some information, directly or indirectly, about the perturbations experiences and actions taken by the other remote controllers; thus allowing local control signals to be modulated accordingly for improving the stability of the entire power system in a distributed manner. This objective of WAC can be achieved in many ways. This study represents a very simple and effective implementation of a WAC for providing additional system damping based on local and remote PSS signals. The structure of the WAC considered in this study is shown in Fig. 4*b*. The wide area monitor senses the local PSS outputs V_{PSSG2}, V_{PSSG3} and V_{PSSG4}. The aggregation of the three modulated PSS outputs is fed back to the AVR exciter inputs connected to each generator by the WAC. The outputs of the WAC for generators G2–G4 are given by V'_{PSSG2}, V'_{PSSG3} and V'_{PSSG4}, respectively. The determination of modulation indices (or weighting factors) for providing coherent damping of

© The Institution of Engineering and Technology 2010

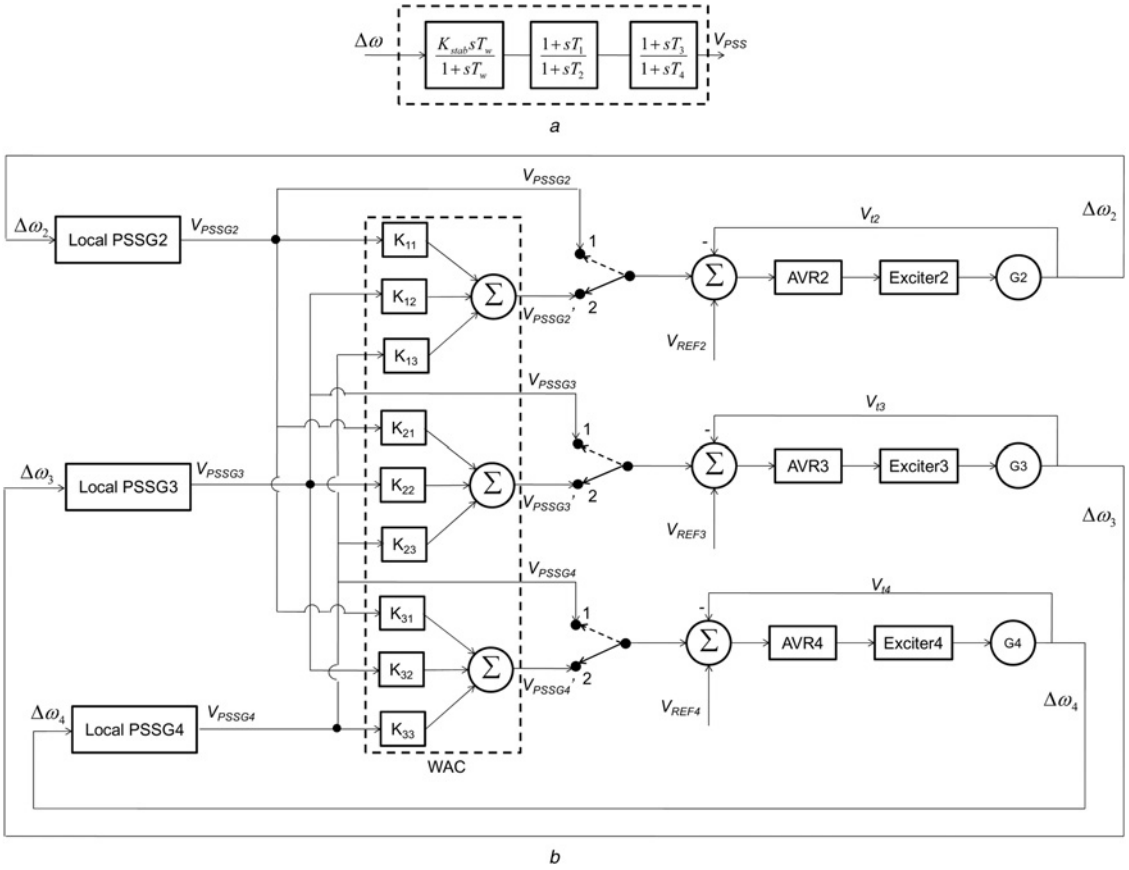

Figure 4 *Power system oscillation damping control system*

a Structure of local PSS
b Structure of the WAC system

low-frequency oscillations in the integrated power system is the critical part in this particular WAC structure. Intelligent tuning of those weighing factors is necessary in order to achieve an overall good control performance. From Fig. 4*b*, it can be seen that there are nine modulation indices to be tuned.

4.2 Tuning of WAC modulation indices

The tuning of modulation indices can be formulated as an optimisation problem. The conventional optimisation algorithms are in most cases derivative or gradient-based algorithms, which are more suitable for deterministic optimisation problems where the function to be optimised can be expressed easily as a differentiable mathematical function of the parameters. But, a power system is a very complex and non-linear system and if all these complexities and non-linearities are included in the mathematical model, the optimisation process becomes computationally very expensive. Besides, it may not be possible to have an accurate mathematical model of a power system. Heuristic algorithms, which do not require a mathematical model of the system and can find the optimum solution based on a non-differentiable objective function, are therefore more effective for this type of optimisation problem involving power systems. There are many types of heuristic algorithms available, for example, genetic algorithm, PSO [19] and differential evolution, which have been successfully used for parameter tuning problems in power system. In this study, PSO is chosen because of its simplicity and easiness of real-time implementation on a DSP.

PSO is a population-based search algorithm modelled after the motion of flock of birds and the school of fishes [19]. A swarm is considered to be a collection of particles, where each particle represents a potential solution to a given problem. The particle changes its position within the swarm based on the experience and knowledge of its neighbours. Basically, it 'flies' over the search space to find out the optimal solution [19]. Initially, a population of random solutions is considered. A random velocity is also assigned to each particle with which its start flying within the search space. Also, each particle has a memory which keeps track of its previous best position and the corresponding fitness. The previous best value is referred to as the 'p_{best}' of a particle. The best of all the 'p_{best}' values is referred to as the 'g_{best}' of the swarm. The fundamental concept of PSO technique is that the particles always accelerate towards their 'p_{best}' and 'g_{best}' positions at each search instant k. The velocity and the position of a particle

© The Institution of Engineering and Technology 2010
IET Gener. Transm. Distrib., 2010, Vol. 4, Iss. 10, pp. 1151–1163
doi: 10.1049/iet-gtd.2009.0505

are updated according to the following equations. The velocity of the ith particle of dth dimension is given by

$$v_{id}(k+1) = wv_{id}(k) + c_1\ \mathrm{rand}_1(p_{\mathrm{best}\_id}(k) - x_{id}(k)) + c_2\ \mathrm{rand}_2(g_{\mathrm{best}\_id}(k) - x_{id}(k)) \quad (1)$$

$$x_{id}(k+1) = x_{id}(k) + v_{id}(k+1) \quad (2)$$

A real-time measurement-based PSO tuning of the WAC weighting factors is implemented on an Innovative Integration M67 DSP card, which is based on the Texas Instruments TMS3206701 processor. The M67 card operates at 160 MHz and is equipped with two A/D and two D/A conversion modules. The rest of the system set-up is built in the RSCAD RTDS software [15]. The analogue signals provided to the M67 are the speed deviations of the generators ($\Delta\omega_2(k)$, $\Delta\omega_3(k)$ and $\Delta\omega_4(k)$), which are taken from the RTDS. These are converted to digital signals through the A/D block of the DSP and are used to calculate the fitness value [explained below and given by (3)] for different combinations of modulation indices. The nine modulation indices ($K_{11}-K_{33}$ as shown in Fig. 4*b*) are the dimensions of each particle of the swarm. The particle positions are initiated randomly inside the DSP. The local PSSs' outputs ($V_{\mathrm{PSSG2}}(k)$, $V_{\mathrm{PSSG3}}(k)$ and $V_{\mathrm{PSSG4}}(k)$) are sent to the DSP to generate the WAC signals for the respective generators ($V'_{\mathrm{PSSG2}}(k)$, $V'_{\mathrm{PSSG3}}(k)$ and $V'_{\mathrm{PSSG4}}(k)$ as shown in Fig. 4*b*. The WAC signals are sent to RTDS as analogue voltage signals in the range of ± 10 V. These voltages are scaled proportionately inside the RTDS and used as the stabilising signals to the AVR and exciter input of each generator at each sampling instant. The calculation of p_{best} and g_{best}, the update of position and velocity, all are performed inside the DSP. The diagram of the laboratory hardware experimental set-up consisting of the RTDS and DSP is shown in Fig. 5.

The PSO algorithm is used to determine optimum values of the modulation indices so that the speed oscillations of the generators are damped quickly. The objective (fitness) function is formulated in such a way that the aforesaid goal is achieved. The mathematical expression of the objective function is as follows

$$J = \sum_{k=1}^{T/\Delta t} \{(\Delta\omega_2(k))^2 + (\Delta\omega_3(k))^2 + (\Delta\omega_4(k))^2\}\Delta t \quad (3)$$

where T is the total time of simulation after the application of a perturbation/disturbance, Δt the sampling interval, k the sampling instant and $\Delta\omega_2(k)$, $\Delta\omega_3(k)$ and $\Delta\omega_4(k)$ are the speed deviations of generators G2, G3 and G4 respectively at kth sampling instant.

For tuning the modulation indices, three disturbances are applied in intervals of 10 s. First, a sudden discharging of the PEVs injecting a total of 120 MW to the system, after that a sudden change from discharging to charging mode absorbing 120 MW from the system and finally, under the last charging mode, a three-phase ten-cycle fault is applied at bus 4. The values of w, c_1 and c_2 in the PSO equation (2) are kept fixed at 0.8, 2.0 and 2.0, respectively, and the number of particles used is 20. These values are chosen based on experience. The optimum modulation indices found after 50 PSO iterations are: $K_{11} = 0.97$, $K_{12} = 0.14$, $K_{13} = 0.08$, $K_{21} = 0.13$, $K_{22} = 1.12$, $K_{23} = 0.21$, $K_{31} = 0.04$, $K_{32} = 0.11$ and $K_{33} = 1.08$.

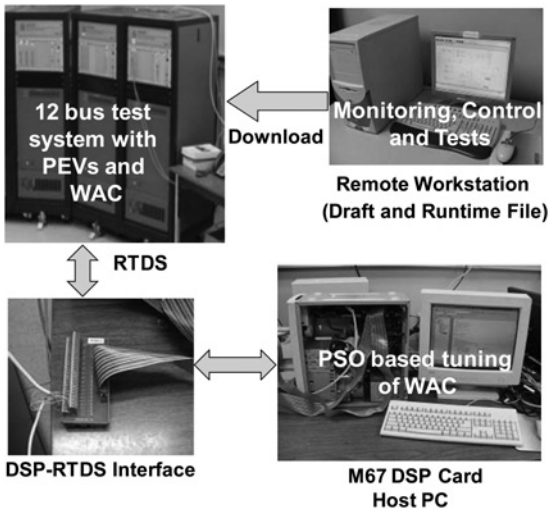

Figure 5 *Laboratory hardware setup*

5 WAC results and discussions

Performance of the WAC is evaluated and compared with performance of the local power system stabilisers under four different disturbances applied to the power system. Among them, the first three (case studies 1–3) are the same disturbances mentioned in Section 4.2 for which the WAC was tuned with PSO. In order to test the robustness of the controller, another disturbance scenario (case study 4) was also studied where the bus 13 parking lots suddenly change their mode from discharging to charging and at the same time the bus 14 parking lots change their mode from charging to discharging. The net active power flow changes from -60 to $+60$ MW in this process. The time domain results and the Prony analysis on the performance of the WAC are given in Sections 5.1 and 5.2, respectively. In Section 5.3, a performance index (PI) is calculated to compare the overall performance of the controllers.

5.1 Case studies

Case study 1: Figs. 6*a*–*c* show the typical speed responses of the generators when the PEV parking lots start discharging. From the figures, it is clear that for all the generators, the overshoots and settling times are less with the WAC in operation. The damping provided by WAC is much better than from the local PSSs only. Figs. 6*d* and *e* show the point of common coupling

© The Institution of Engineering and Technology 2010

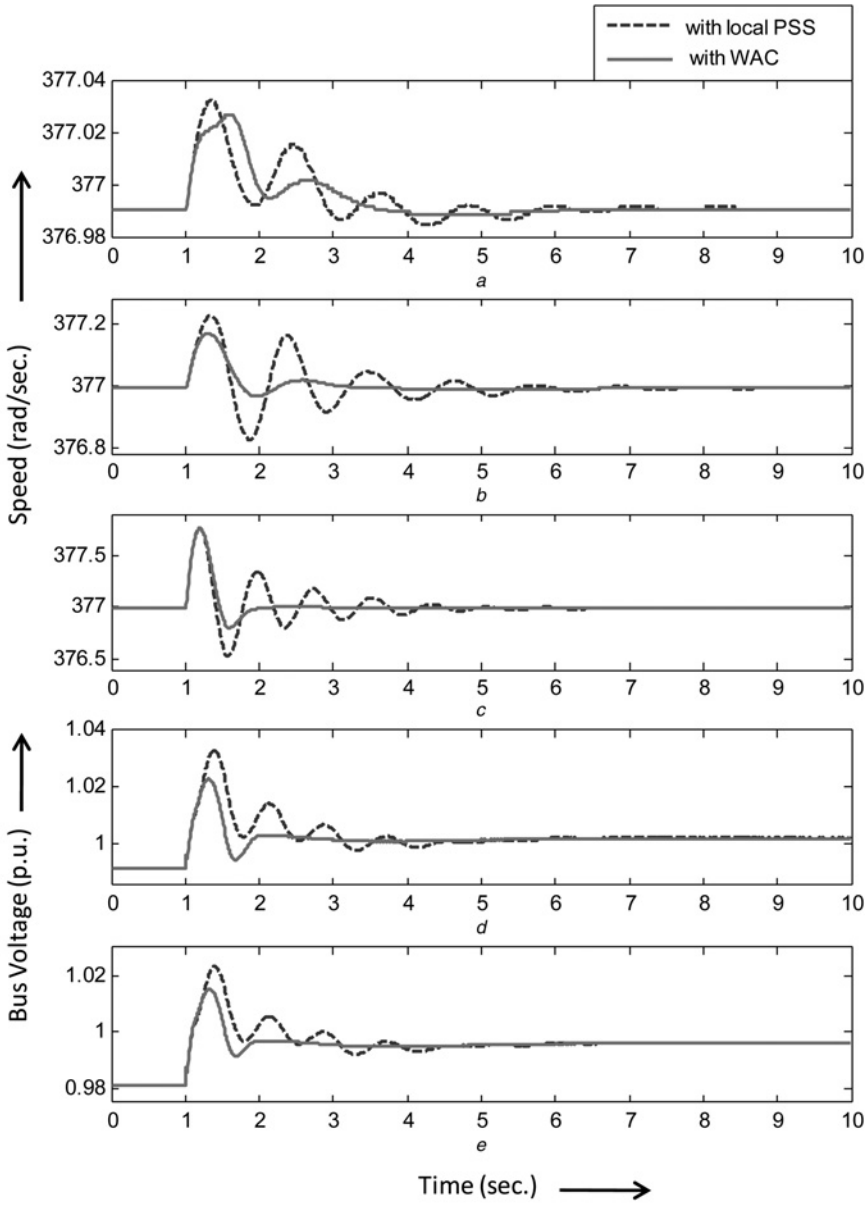

Figure 6 *Impact of sudden discharging of the PEV parking lots with and without WAC*

a Speed oscillation of G2
b Speed oscillation of G4
c Speed oscillation of G3
d Voltage oscillation at bus 14
e Voltage oscillation at bus 13

voltages at buses 14 and 13, respectively. It is observed that the WAC plays a very good role to settle down the voltage oscillations quickly and thus outperformed the local PSS performances.

Case study 2: Figs. 7*a*–*c* show the speed responses of the generators for the second disturbance when the parking lots suddenly switch their modes of operation from discharging to charging. Here again, it is observed that the performance of the WAC is much superior to the local PSS. The bus voltage characteristics presented by Figs. 7*d* and *e* also show that the damping is improved with the addition of WAC.

Case study 3: A ten-cycle three phase to ground fault with duration ten cycles is applied to bus 4. The speed and bus voltage characteristics are shown in Fig. 8. Here also the performance of the WAC in damping the speed oscillations is superior to the local PSS for all the generators and the performances of the WAC and the local PSS are the same for voltage oscillations at buses 13 and 14.

Case study 4: The weights of the WAC were not tuned by PSO for this disturbance. Still it is observed in Figs. 9*a*–*c* that all the generator speed oscillations are damped quite fast with the WAC. The bus voltage oscillations, as observed from Figs. 9*d* and *e*, are also damped out earlier.

© The Institution of Engineering and Technology 2010

doi: 10.1049/iet-gtd.2009.0505

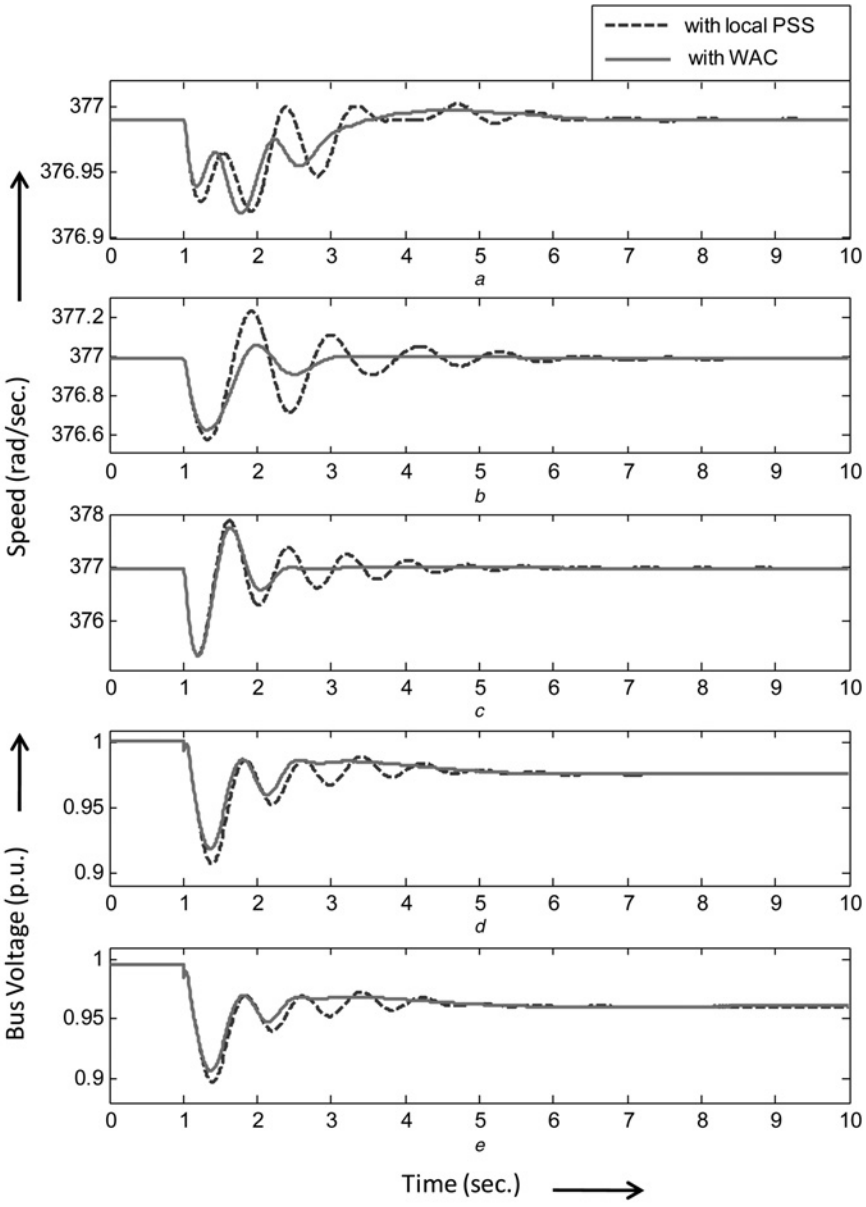

Figure 7 *Impact of sudden transition from discharging to charging of the PEV parking lots with and without WAC*

a Speed oscillation of G2
b Speed oscillation of G4
c Speed oscillation of G3
d Voltage oscillation at bus 14
e Voltage oscillation at bus 13

In order to quantify the stability improvements seen with the WAC, Prony analysis is performed on the time domain results to determine the frequency modes and the corresponding damping ratios.

5.2 Stability analysis with the Prony method

Prony analysis [20] is an extension of Fourier analysis and it helps to find the modal contents by estimating frequency, damping and phase of a signal. This analysis tool is useful to provide information on the stability of the system at the operating point of concern without any need of extensive technique for linearisation of the complete system model. The analysis is performed on the measured data; hence no prior information regarding the system is required. The real-time implementation platform consisting RTDS and DSP does not provide any means to obtain the linearised closed-loop model of the system. Therefore to illustrate and quantify the improvement with the WAC design in terms of damping ratios, the Prony method is chosen. This method is applied on the speed data of generator G4. The frequency and damping of each dominant mode is given in Tables 2–5. It is observed that the system has three dominant local modes of oscillations: the first one in the range of 0.88–0.89 Hz, the second one in the range of

© The Institution of Engineering and Technology 2010

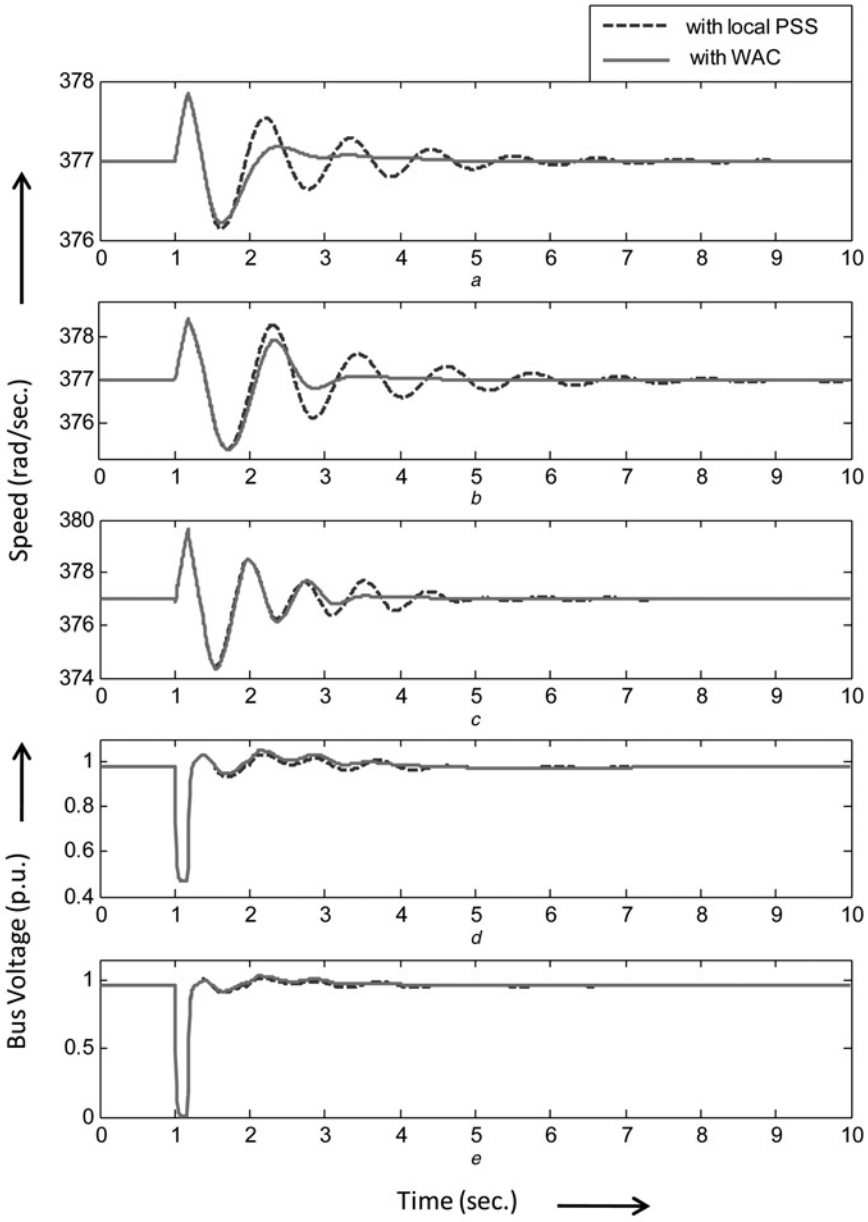

Figure 8 *Impact of a three phase ten-cycle fault at bus 4 in charging mode*

a Speed oscillation of G2
b Speed oscillation of G4
c Speed oscillation of G3
d Voltage oscillation at bus 14
e Voltage oscillation at bus 13

0.92–0.93 Hz and the third one in the range of 1.26–1.28 Hz approximately. For all of these three modes, the damping ratio of the system with local PSSs is found to be more than that of the system without PSS. Similarly, the damping ratio of the system with the WAC is again higher than the system with local PSSs. For example, in case study 2 (Table 3), the Prony analysis shows that the generator G4 has three dominant local modes of frequencies 0.8880, 0.9228 and 1.2609 Hz without PSS. The corresponding damping ratios are 0.0442, 0.0151 and 0.0425, respectively. With PSS, the corresponding damping ratios are 0.1611, 0.0781 and 0.0865, respectively, which are higher than the system without PSS. Similarly, with the WAC, the damping ratios are 0.3220, 0.1435 and 0.2144, respectively. This is of course significantly higher than the system with PSS.

Another possible advantage of WAC is that, the required system damping (greater than 5%) can be achieved even without a local PSS. In order to establish this, the system performance under case study 1 with WAC and two local PSSs instead of three is studied. Among all the possible combination of two local PSSs, it is observed that the combination of PSS at G2 and G3 (excluding the PSS at G4) gives the best performance. The Prony analysis of this case study is presented in Table 6. It is observed that the

© The Institution of Engineering and Technology 2010

doi: 10.1049/iet-gtd.2009.0505

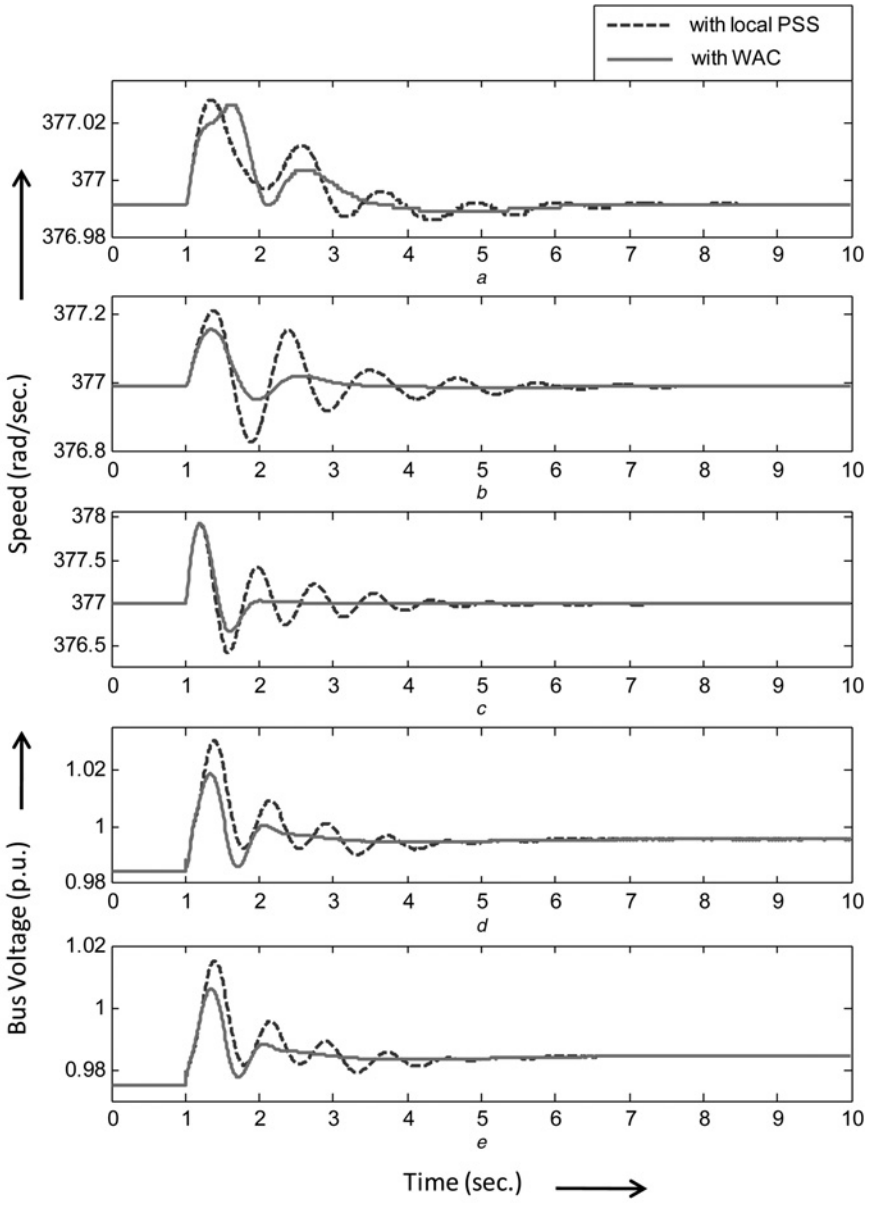

Figure 9 *Impact of sudden transition from discharging to charging for PL1 and PL2 and charging to discharging for PL3–PL8*

a Speed oscillation of G2
b Speed oscillation of G4
c Speed oscillation of G3
d Voltage oscillation at bus 14
e Voltage oscillation at bus 13

Table 2 Frequency and damping of the system under case study 1

	No PSS		With PSS		With WAC	
	f, Hz	ζ	*f*, Hz	ζ	*f*, Hz	ζ
G4	0.8808	0.0080	0.8812	0.1121	0.8801	0.2017
	0.9310	0.0333	0.9297	0.0981	0.9312	0.3001
	1.2679	0.0221	1.2641	0.0803	1.2701	0.2543

Table 3 Frequency and damping of the system under case study 2

	No PSS		With PSS		With WAC	
	f, Hz	ζ	*f*, Hz	ζ	*f*, Hz	ζ
G4	0.8880	0.0442	0.8869	0.1611	0.8891	0.3220
	0.9228	0.0151	0.9214	0.0781	0.9234	0.1435
	1.2609	0.0425	1.2598	0.0865	1.2621	0.2144

© The Institution of Engineering and Technology 2010

Table 4 Frequency and damping of the system under case study 3

	No PSS		With PSS		With WAC	
	f, Hz	ζ	*f*, Hz	ζ	*f*, Hz	ζ
G4	0.8911	0.0320	0.8920	0.1424	0.8905	0.3457
	0.9322	0.0411	0.9334	0.0911	0.9308	0.2010
	1.2801	0.0288	1.2796	0.1062	1.2789	0.2931

Table 5 Frequency and damping of the system under case study 4

	No PSS		With PSS		With WAC	
	f, Hz	ζ	*f*, Hz	ζ	*f*, Hz	ζ
G4	0.8907	0.0294	0.8912	0.0682	0.8894	0.2000
	0.9293	0.0104	0.9300	0.0561	0.9282	0.1743
	1.2766	0.0437	1.2741	0.1514	1.2719	0.3441

Table 6 Performance comparison between WAC with two local PSSs and WAC with three local PSSs

	WAC with three local PSSs		WAC with two local PSSs	
	f, Hz	ζ	*f*, Hz	ζ
G4	0.8801	0.2017	0.8814	0.0515
	0.9312	0.3001	0.9296	0.2944
	1.2701	0.2543	1.2689	0.0643

damping of two local modes with frequencies 0.88 and 1.27 Hz are just above 5% and the damping of the mode with frequency 0.93 Hz is close to 30%. This performance is compared with a system where WAC as well as all the three local PSSs are present. Obviously, the performance for WAC with three local PSSs is much superior to WAC with two local PSSs. Since this 12-bus system under study only has dominant local modes instead of inter-area modes, it is therefore very difficult for the WAC to achieve a very good performance without the presence of any one of the local PSSs, although the system can still achieve the required damping (greater than 5%) with the reduced number of PSSs in presence of WAC.

5.3 Performance index from transient energy

In this section, the performance of the local PSSs and the WAC are compared in terms of transient energies. When a disturbance occurs in a power system, the transient energy injected into the system can cause it to go unstable if the controller does not provide sufficient damping. Therefore a properly tuned damping controller is required to minimise the transient energy injected into the system for various disturbances.

Table 7 Normalised performance index for four case studies

	Case 1	Case 2	Case 3	Case 4	Overall
no PSS	1	1	1	1	1
local PSS	2.252	2.1613	3.0581	2.1828	2.2280
WAC	3.7724	2.7742	3.6697	3.4194	3.5200

For the four case studies mentioned in this study, the sum of transient energies of generators G2–G4 for the first 9 s after the disturbances are calculated [$T = 9$ s, given in (4)] according to the following equation

$$\mathrm{TE} = \sum_{t=t_s}^{t_f} 0.5 * \{H_2 * (\Delta w_2(k))^2 + H_3 * (\Delta w_3(k))^2 + H_4 * (\Delta w_4(k))^2\} \quad (4)$$

where H_2, H_3 and H_4 are the inertias of generators G2, G3 and G4, respectively. The performance of the system without PSS, with local PSSs and with WAC are compared by defining PI given in

$$\mathrm{PI} = \frac{1}{\mathrm{TE}} \quad (5)$$

Table 7 shows the performance comparisons for the four case studies. The PIs are normalised by dividing the PIs by that PI obtained without PSS. Owing to this type of representation, a higher value of PI indicates a better performance. From Table 7, it is clearly observed that the PI is much higher with WAC than the local PSSs for all the case studies.

Therefore from both time-domain and Prony analysis results and also from the transient energy-based PI calculations, it can be concluded that the designed WAC has the potential to improve the stability of a power system when the PEV-based parking lots are in operation and bulk transactions are carried out.

6 Conclusions

A real-time RTDS model of a fleet of plug-in vehicles performing V2G power transactions has been presented in this study. Eight parking lot models, each with a capacity for 800 vehicles and ± 20 MW power transaction capability, are connected to the grid and the impact of their bulk level charging and discharging transients have been evaluated. In order to improve the stability of the integrated power system with PEVs, a simple and an effective WAC structure has been designed for the system. A real-time PSO-based tuning method is adopted which runs on a DSP in synchronism with the integrated power system simulated on

© The Institution of Engineering and Technology 2010

doi: 10.1049/iet-gtd.2009.0505

the RTDS platform. It is observed that a properly tuned WAC can damp out the oscillations caused by the sudden switching charging and discharging modes of the PEVs much quicker than generators equipped with local PSSs only.

The future work can focus on both macro and micro levels of control. In the micro level, the impact of the transients and grid faults on the individual inverters of the PEVs can be studied. This will eventually lead to the protection aspects for the PEVs. In the macro level, the development of an adaptive WAC which can modify the control actions online based on the nature of the disturbance and time delays in the remote signal transmissions.

7 Acknowledgment

The financial support from the National Science Foundation, USA, under the EFRI Project no. 0836017 is gratefully acknowledged by the authors.

8 References

[1] KEMPTON W., TOMIĆ J.: 'Vehicle-to-grid power fundamentals: calculating capacity and net revenue', *J. Power Sources*, 2005, **144**, (1), pp. 268–279

[2] AC Propulsion: 'AC-150 EV power system', http://www.acpropulsion.com/tzero/AC150_Gen2_specs.pdf

[3] NI H., HEYDT G.T.: 'Power system stability agents using robust wide area control', *IEEE Trans. Power Syst.*, 2002, **17**, (4), pp. 1123–1131

[4] TAYLOR C.W., ERICKSON D.C., MARTIN K.E., WILSON R.E., VENKATASUBRAMANIAN V.: 'WACS-wide area stability and voltage control system: R & D and online demonstartion', *Proc. IEEE*, 2005, **93**, (5), pp. 892–906

[5] KAMWA I., GRONDIN R.: 'PMU configuration for system dynamic performance measurement in large, multiarea power systems', *IEEE Trans. Power Syst.*, 2002, **17**, (2), pp. 385–394

[6] ABOUL-ELA M.E., SALLAM A.A., MCCALLEY J.D., FOUAD A.A.: 'Damping controller design for power system oscillations using global signals', *IEEE Trans. Power Syst.*, 1996, **11**, pp. 767–773

[7] RAY S., VENAYAGAMOORTHY G.K.: 'Real-time implementation of a measurement based adaptive wide area control system considering communication delays', *IET Gener. Transm. Distrib.*, 2008, **1**, (2), pp. 62–70

[8] OKOU F., DESSAINT L.A., AKHRIF O.: 'Power systems stability enhancement using a wide-area signals based hierarchical controller', *IEEE Trans. Power Syst.*, 2005, **20**, (3), pp. 1465–1477

[9] SNYDER A.F., IVANESCU D., HADJSAID N., GEORGES D., MARGOTIN T.: 'Delayed-input wide area stability control with synchronized phasor measurements and linear matrix inequalities', IEEE Power Engineering Society Summer Meeting, 2000, vol. 2, pp. 1009–1014

[10] HONGXIA W., HEYDT G.T.: 'Design of delayed-input wide area power system stabilizer using the gain scheduling method'. IEEE Power Engineering Society General Meeting, 2003, vol. 3, pp. 1704–1709

[11] CHAUDHURI B., MAJUMDER R., PAL B.C.: 'Wide-area measurement-based stabilizing control of power system considering signal transmission delay', *IEEE Trans. Power Syst.*, 2004, **19**, (4), pp. 1971–1979

[12] QIAO W., VENAYAGAMOORTHY G.K., HARLEY R.G.: 'Optimal wide-area monitoring and non-linear adaptive coordinating control of a power system with wind farm integration and multiple FACTS devices', *Neural Netw.*, 2008, **21**, (2–3), pp. 466–475

[13] MOHAGHEGHI S., VENAYAGAMOORTHY G.K., HARLEY R.G.: 'Optimal wide area controller and state predictor for a power system', *IEEE Trans. Power Syst.*, 2007, **22**, (2), pp. 693–705

[14] JIANG S., ANNAKKAGE U.D., GOLE A.M.: 'A platform for validation of FACTS models', *IEEE Trans. Power Deliv.*, 2006, **21**, pp. 484–491

[15] FORSYTH P., MAGUIRE T., KUFFEL R.: 'Real time digital simulation for control and protection system testing'. IEEE 35th Annual Power Electronics Specialists Conf., 2004, vol. 1, pp. 329–335

[16] KRAUSE P.C., WASYNCZUK O., SUDHOFF S.D.: 'Analysis of electric machinery and drive systems' (IEEE Press, 2002)

[17] HUTSON C., VENAYAGAMOORTHY G.K., CORZINE K.: 'Intelligent scheduling of hybrid and electric vehicle storage capacity in a parking lot for profit maximization in grid power transactions'. IEEE Energy 2030, Atlanta, GA, USA, 17–18 November 2008

[18] SABER A.Y., VENAYAGAMOORTHY G.K.: 'Intelligent unit commitment with vehicle-to-grid – a cost-emission optimization', *J. Power Sources*, 2010, **195**, (3), pp. 898–911

[19] DEL VALLE Y., VENAYAGAMOORTHY G.K., MOHAGHEGHI S., HERNANDEZ J., HARLEY R.G.: 'Particle swarm optimization: basic concepts, variants and applications in power system', *IEEE Trans. Evol. Comput.*, 2008, **12**, (2), pp. 171–195

[20] HAUER J.F.: 'Application of Prony analysis to the determination of modal content and equivalent models for measured power system response', *IEEE Trans. Power Syst.*, 1991, **6**, (3), pp. 1062–1068

© The Institution of Engineering and Technology 2010